

Multi-Branch Fully Convolutional Network for Face Detection

Yancheng Bai
KAUST

yancheng.bai@kaust.edu.sa

Bernard Ghanem
KAUST

bernard.ghanem@kaust.edu.sa

Abstract

Face detection is a fundamental problem in computer vision. It is still a challenging task in unconstrained conditions due to significant variations in scale, pose, expressions, and occlusion. In this paper, we propose a multi-branch fully convolutional network (MB-FCN) for face detection, which considers both efficiency and effectiveness in the design process. Our MB-FCN detector can deal with faces at all scale ranges with only a single pass through the backbone network. As such, our MB-FCN model saves computation and thus is more efficient, compared to previous methods that make multiple passes. For each branch, the specific skip connections of the convolutional feature maps at different layers are exploited to represent faces in specific scale ranges. Specifically, small faces can be represented with both shallow fine-grained and deep powerful coarse features. With this representation, superior improvement in performance is registered for the task of detecting small faces. We test our MB-FCN detector on two public face detection benchmarks, including Fddb and WIDER FACE. Extensive experiments show that our detector outperforms state-of-the-art methods on all these datasets in general and by a substantial margin on the most challenging among them (e.g. WIDER FACE Hard subset). Also, MB-FCN runs at 15 FPS on a GPU for images of size 640×480 with no assumption on the minimum detectable face size.

1. Introduction

Face detection is a fundamental and important problem in computer vision, since it is usually a key step towards many subsequent face-related applications, including face parsing, face verification, face tagging and retrieval, etc. Face detection has been widely studied over the past few decades and numerous accurate and efficient methods have been proposed for mostly constrained scenarios. Recent works focus on faces in uncontrolled settings, which is much more challenging due to the significant variations in illumination, pose, scale and expressions. A thorough survey on face detection methods can be found in [35].



Figure 1. Example detection results generated by our proposed MB-FCN face detector. It can handle faces with large scale variations, extreme pose, exaggerated expressions, and occlusion with only a single pass through the backbone network. Bounding boxes with a green and red color are ground-truth annotations and MB-FCN detection results, respectively.

Face detection is the task of finding the locations of all faces in an image with arbitrary sizes. As shown in Figure 1, the scale variations may be significant. To deal with this problem, both traditional face detectors [27, 4, 29] and CNN-based ones [13, 28, 40] have to exhaustively search for faces on different levels of an image pyramid constructed from the original image. This constitutes the main computational bottleneck of many modern face detectors, which prohibit their use in a vast range of realtime real-world applications. Moreover, small faces tend to require higher-resolution features for discrimination and effective localization. However, most CNN-based detectors represent targets by only exploiting the deep coarse features, which lose most spatial information of small faces due to the down-

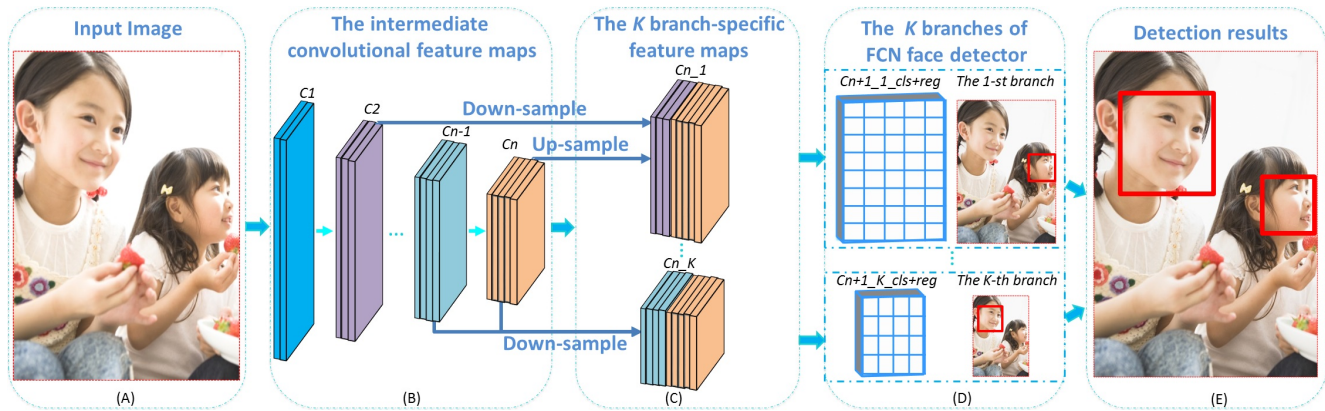


Figure 2. The pipeline of the proposed multi-branch FCN face detector system. (A) Testing images are fed to the network; (B) After several layers of convolution, a series of *conv* feature maps at several scales are generated; (C) Scale specific skip connections of *conv* feature maps generate K specific feature maps for each branch to represent faces at specific scale ranges; (D) Each FCN operates on its specific feature maps and outputs classification (*cls*) and regression (*reg*) results; (E) The *cls* and *reg* outputs are converted into scored bounding boxes, and non-maximum suppression (NMS) is applied to all bounding boxes of all branches to obtain the final detection results.

sampling operations. This prohibits accurate localization of these types of challenging faces, which is reflected in the substantial state-of-the-art performance disparity between the detection of small vs. large faces.

In this paper, we aim to propose a face detector, whose design takes into consideration both computational efficiency and effectiveness. Regarding efficiency, we propose a multi-branch fully convolutional neural network architecture (MB-FCN), in which each branch is a FCN trained for detecting faces within specific scale ranges. And the MB-FCN detector can deal with faces at all scales in an image, while only requiring a single pass through the network. Compared to passing through each level of an image pyramid, our MB-FCN model can save computational resources and therefore is more efficient. Regarding effectiveness, we enable skip connections of the convolutional (*conv*) feature maps at different layers to represent faces in specific scale ranges. Specifically, small faces are represented with both shallow (spatially fine-grained) and deep (spatially coarse) features. In our experiments, we demonstrate that this representation is very important in achieving superior performance, especially on small faces.

Contributions. This paper makes three main contributions. (1) A new multi-branch FCN architecture for face detection is proposed, where each branch is a FCN trained to handle faces in specific ranges. More importantly, the MB-FCN detector can detect faces within all scale ranges in images with a single pass. (2) Scale specific skip connections of different layers are exploited for each branch, which can represent faces within specific ranges much better than only using the final *conv* feature maps, especially for faces at small scales. (3) The MB-FCN detector outperforms state-of-the-art methods on two popular benchmarks, where the most impressive improvement occurs in the most challeng-

ing subset of these datasets. Also, MB-FCN is computationally efficient with a runtime of 15 FPS on a GPU for 640×480 images and with no assumption on the minimum detectable face size.

2. Related Work

2.1. Handcrafted Feature Based Face Detection

As a classic topic, numerous face detection systems have been proposed during the past decade or so. Building an effective and efficient detector is the ultra goal of detection system designers. Since the seminal work of Viola and Jones (VJ) [27], the boosting cascade framework has become the *de facto* standard for rapid object detection. The attentional cascade structure is the critical component for the success of the VJ framework. The key insight is that smaller but more efficient classifiers can be learned, which can reject the majority of negative sub-windows, while keeping almost all positive examples. Consequently, most of the sub-windows will be rejected in early stages of the detector, making the system extremely efficient. However, due to the limited representation of Haar-like features, the original VJ detector shows poor performance in uncontrolled environments. HOG [5], SURF [17] and other sophisticated features [31] have been exploited to enrich the capacity of feature representation, and thus improve detection performance.

A similar idea has also been applied to cascaded deformable parts model (DPM) [30, 29], which is another traditional paradigm for object detection. In each stage of the cascade DPM detector, a hypothesis can be pruned if its score is below a pre-learned threshold. Therefore, this can reduce the number of parts evaluated and accelerate the evaluation process without sacrificing detection accuracy.

However, most of the detection systems based on hand-crafted features only train a single scale model, which is applied to each level of a feature pyramid, thus, increasing the computational cost drastically, especially for complicated features. More importantly, the limited representation of hand-crafted features restricts the performance of detectors, particularly in uncontrolled settings.

2.2. CNN-Based Face Detectors

In recent years and motivated by the superior performance of CNNs for image classification and scene recognition [15, 25, 39], generic object detectors based on CNNs, *e.g.*, the Region-based CNN (RCNN) [8], Faster RCNN [23] and its other variants have been introduced [8, 7, 23] and they achieve state-of-the-art detection performance. Specifically, Faster RCNN [23] has recently achieved a balance between both detection performance and computational efficiency. In fact, it has become the *de facto* framework for general object detection.

Inspired by the great success of Faster RCNN, several recent works [13, 28, 40] have utilized this framework to detect faces and shown impressive performance on the FDDB benchmark [11]. However, performance drops dramatically on the more challenging WIDER FACE dataset [33], which contains a large number of faces with lower resolution. The main reason for this disparity is that deep *conv* feature maps with lower spatial resolution are used for representation, which is insufficient for handling small faces [38, 2]. To overcome this problem, detectors [13, 28, 40] have to up-sample input images during training and testing, which inevitably increases memory and computation costs. Compared to these methods, our detector exploits the intermediate *conv* feature maps with higher resolution to deal with small faces, making the process more efficient.

To deal with the efficiency problem, Li *et al.* [16] propose a cascaded architecture for real-world face detection inspired by the success of boosting-based algorithms [27]. Two lower-resolution models are used to quickly reject most hypothesis windows and higher resolution models are applied to get the final detection results. A multi-task variant of [16] for face detection and alignment is proposed in [37]. However, each stage in [16, 37] needs to be tuned carefully and is trained separately. To overcome this problem, a joint training variant is proposed in [22]. However, all these methods have an assumption on the minimum resolution of detected faces. Decreasing the minimum resolution quickly increases the runtime of these methods.

Compared to these methods, our detector learns multi-branch models to detect faces of all scales with a single pass through the backbone network. Hence, our detector is more effective. Unlike other methods, faces with lower spatial resolution (prevalent in the WIDER FACE dataset and in real-world applications) will not be missed by our detector,

since it does not make any assumption on the minimum scale of faces to be detected.

2.3. Multi-Branch Generic Detectors

The works of [19, 2] employ intermediate *conv* feature maps with fine resolution to represent small objects and learn multi-scale models to detect small objects in a single shot. There are some common design aspects between their CNN architecture and ours. However, our method detects small objects by combining both shallow (spatially fine-grained) feature maps with deep and powerful (spatially low resolution) feature maps, which shows significant improvements over these two works [19, 2]. Moreover, we empirically show that adding more branches in [19, 2] might not increase the performance of face detection.

2.4. Skip Connection Representation

Small objects in images require fine scale representation. Skip connections [9, 1, 36] have been proposed for this purpose, which combines fine-grained *conv* feature maps from shallow layers and coarse semantic features from deep layers to represent objects more precisely. However, simply incorporating all feature maps from different layers may not yield performance improvement. In fact, increasing these skip connections might decrease detection performance in some cases. Unlike these previous methods, we make a thorough analysis of this design aspect to find the best skip connections for each branch in our face detection network.

3. Multi-Branch FCN Model

In this section, we will introduce our deep architecture for multi-branch FCN face detection and then give a detailed description on how to implement it.

3.1. Overview of Architecture

As illustrated in Figure 2, the whole architecture consists of four components. **(i)** The first component is the shared intermediate *conv* layers, which can be of any typical architecture like AlexNet [15], VGGNet [25] or ResNet [10]. In our experiments, ResNet-50 [10] pre-trained on the ImageNet dataset is adopted as the backbone network. After images are passed through the backbone network, the *conv* feature maps of every layer are generated. **(ii)** The second component creates the skip connections of feature maps at different scales to represent targets of different resolutions for every branch. Up-sampling and down-sampling operate on the *conv* feature maps of different scales to produce K -branch feature maps. Using this implicit multi-scale feature construction strategy can save a substantial amount of computational cost compared to explicitly re-sampling images, which have to pass through the backbone network several times. **(iii)** For each branch, multi-task learning is deployed to learn one FCN to deal with faces within certain

scales. Specifically, each FCN takes as input a 1×1 spatial window of the input convolutional feature map, and outputs a lower-dimensional feature, which is fed into two sibling fully-connected layers (*reg* and *cls*) with filter size 1×1 . (iv) The *reg* and *cls* outputs of every branch are converted to scored bounding boxes. Then, non-maximum suppression (NMS) is applied to those with confidence above a predefined threshold, and the final detection results are obtained.

3.2. Branch-Specific Skip Connection

In the forward pass, the backbone network computes a series of *conv* feature maps at several scales with a scaling step of 2. For clarity, we denote these feature maps as $\{C2, C3, C4, C5\}$ for conv2, conv3, conv4, and conv5 outputs of ResNet-50. The original stride of ResNet-50 is 32, which makes the final *C5* feature maps too coarse. To increase the resolution of the *C5* feature maps, we reduce the effective stride from 32 pixels to 16 pixels as done in [14]. Consequently, their corresponding strides of each layer are $\{4, 8, 16, 16\}$ pixels with respect to the input image.

In fact, 50% of faces in the WIDER FACE dataset have an area less than 32×32 or even 16×16 pixels, so these objects will have been down-sampled to 2×2 or 1×1 at the *C5* stage. Clearly, if this happens, most spatial information will have been lost due to the effective 16 time down-sampling. Therefore, skip connections are needed to guarantee the classifier access to information from features at multiple spatial resolutions. This will especially help detect small faces. To deal with different resolutions of different *conv* feature maps, deconvolution [20] using fixed bilinear interpolation weights and max pooling are used for up-sampling and down-sampling in our current implementation. We can also design other more complicated skip connection modules, however, these will inevitably sacrifice computational efficiency.

In our architecture, there are K branches to deal with faces at different scales. Should we simply connect all the *conv* outputs *C2, C3, C4, C5* to every branch? Obviously, it would be sub-optimal. First, it will increase the computational burden. Second, simply skipping connection of all intermediate *conv* maps might decrease the performance due to over-fitting caused by the curse of dimensionality. For example, the less powerful *C2* feature maps might be useless for faces of large scales, though its fine information might be essential in representing faces at lower resolution. Therefore, we need to find the best skip connections for each branch considering both efficiency and effectiveness. Interestingly, the architectures of MSCNN [2] and SSD [19] can be seen as a special version of our architecture, if there are no skip connections for each branch.

3.3. Multi-Branch Multi-Task Training

The k -th branch FCN has two sibling output layers, *cls* and *reg*. The *cls* layer computes the confidence score y_{ki} of the i -th anchor at the k -th branch, where an anchor denotes a candidate box associated with a scale and aspect ratio [23]. The score y_{ki} represents whether the corresponding anchor shows a face or not. Given the ground truth label $y_{ki}^* \in \{0, 1\}$, the softmax loss for classification is defined as follows:

$$L_{cls}(y_{ki}, y_{ki}^*) = y_{ki}^* \log(y_{ki}) + (1 - y_{ki}^*) \log(1 - y_{ki}) \quad (1)$$

The *reg* layer generates the 4 parameterized coordinates of the predicted bounding box $\mathbf{p}_{ki} = [p_x, p_y, p_w, p_h]_{ki}$, corresponding to its left corner, width, and height. Moreover, we represent the ground-truth box $\mathbf{p}_{ki}^* = [p_x^*, p_y^*, p_w^*, p_h^*]_{ki}$ associated with anchor i of branch k . We utilize the standard regression loss proposed in [7], which is defined as follows:

$$L_{loc}(\mathbf{p}_{ki}, \mathbf{p}_{ki}^*) = \sum_{j \in \{x, y, w, h\}} \text{smooth}_{L_1}(\mathbf{p}_{ki}^* - \mathbf{p}_{ki})_j, \quad (2)$$

where

$$\text{smooth}_{L_1}(x) = \begin{cases} \frac{x^2}{2} & \text{if } |x| < 1 \\ |x| - 0.5 & \text{otherwise} \end{cases} \quad (3)$$

is a robust L_1 loss that is less sensitive to outliers than the L_2 loss. With these definitions, we can minimize the following multi-branch multi-task loss L of anchors on the *conv* feature maps to jointly train for classification and bounding-box regression:

$$L(\mathbf{y}, \mathbf{p}) = \sum_{k=1}^K \gamma_k \sum_{i=1}^N (L_{cls}(y_{ki}, y_{ki}^*) + \lambda_k y_{ki}^* L_{loc}(\mathbf{p}_{ki}, \mathbf{p}_{ki}^*)) \quad (4)$$

where $\mathbf{y} = [y_{1i}, \dots, y_{1N}, \dots, y_{Ki}, \dots, y_{KN}]$ and $\mathbf{p} = [\mathbf{p}_{1i}, \dots, \mathbf{p}_{1N}, \dots, \mathbf{p}_{Ki}, \dots, \mathbf{p}_{KN}]$ denote the vectors of predicted labels and bounding boxes of the corresponding anchors, respectively. N denotes the mini-batch size. γ_k balances the importance of models at different branches. In our experiments, each γ_k is set to 1, which means that all K models carry the same importance. This can be changed to reflect the scale statistics of faces in the training data. The term $y_{ki}^* L_{loc}(\mathbf{p}_{ki}, \mathbf{p}_{ki}^*)$ means that the regression loss is activated only for positive anchors (*i.e.* when $y_{ki}^* = 1$) and is disabled otherwise. For background anchors, there is no notion of a ground-truth bounding box and hence L_{loc} is ignored. λ_k is the tradeoff parameter between classification and localization. In our experiments, we set to $\lambda_k = 2 \forall k$ to encourage better localization.

3.4. Implementation Details

Training setup. We use the large-scale WIDER FACE dataset [33] to train our MB-FCN detector. During training, each mini-batch is constructed from one image, chosen uniformly at random from the training dataset. To fit it in GPU memory, the image is resized by the ratio $1024/\max(w, h)$, where w and h are its width and height, respectively.

An anchor is assigned with a positive label, if the intersection over union (IoU) overlap between it and any ground-truth bounding box is larger than 0.55; otherwise, it is negative if the maximum IoU with any ground-truth face is less than 0.35. We also employ data augmentation by horizontally flipping each image per batch with a probability of 0.5.

Optimization. Our MB-FCN model is a fully convolutional network [20], which can be trained end-to-end by back-propagation and stochastic gradient descent (SGD). We follow the image-centric training strategy from [7, 23] in training. Each mini-batch contains many positive and negative examples that are sampled from a single image. Obviously, negative samples will dominate, which will lead to biased prediction, if they are all used to compute the loss function. To avoid this bias and to speedup training, we employ the hard negative example mining strategy in [14, 24], where different sets of negative samples are chosen in each iteration based on their loss using the most recently trained network.

Hyper-parameters. The weights of the filters of all layers (except for the shared ones) are initialized by randomly drawing from a zero-mean Gaussian distribution with standard deviation 0.01. Biases are initialized at 0.1. All other layers are initialized using a model pre-trained on ImageNet. The same mini-batch size of 128 is employed for each branch in MB-FCN. The learning rate is initially set to 0.001 and then reduced by a factor of 10 after every 30k mini-batches. Training is terminated after a maximum of 80k iterations. We also use a momentum of 0.9 and a weight decay of 0.0005. Our system is implemented in Caffe [12] and its source code will be made publicly available.

4. Experiments

In this section, we will experimentally validate our proposed method. Firstly, we dive into the details to find the best skip connections for each branch and the optimal number of branches for our detector. Secondly, we evaluate the proposed MB-FCN detector on two public face detection benchmarks, including WIDER FACE [33] and FDDB [11], while comparing it against state-of-the-art detectors.

4.1. Training and Validation Datasets

To train our multi-branch FCN detector, we use a recently released large-scale face detection benchmark, the WIDER FACE dataset [33]. It contains 32,203 images, which are selected from the publicly available WIDER

dataset. And 40%/10%/50% of the data is randomly selected for training, validation, and testing, respectively. There are 393,703 labeled faces with a high degree of variability in scale, pose, occlusion, expression, appearance, and illumination. Images in WIDER FACE are categorized into 61 social event classes, which have much more diversity and is closer to what is encountered in real-world applications. Therefore, we use this dataset for training and validating our models under different parameter settings.

In fact, the WIDER FACE dataset is divided into three subsets: Easy, Medium, and Hard, based on the heights of the ground truth faces [33]. The Easy/Medium/Hard subsets contain faces with heights larger than 50/30/10 pixels respectively. Compared to the Medium subset, the Hard one contains many faces with height between 10 – 30 pixels. As expected, it is quite challenging to achieve good detection performance on the Hard subset.

4.2. What are the best skip connections for each branch?

Skip connections combine the intermediate *conv* feature maps for precise representation of objects, especially those with small spatial resolution. However, connecting all these maps together will likely make the detector inefficient and the avoidance of over-fitting challenging. As such, we seek the optimal connections for each branch. To do this, we first seek the best combination of connections for each single branch separately. Then, we perform a greedy strategy that loops over each branch optimizing its best connections while keeping the other connections the same. In doing so, we are iteratively improving the overall detection performance while greedily adding connections to the different branches. First, we summarize the detection results for the single branch models in Table 1, in which case they are applied independently. It is clear that each of these models achieves impressive validation performance on all subsets of WIDER FACE dataset [33], especially when compared to three state-of-the-art face detectors [33, 37, 40]. In fact, the C5(16) model, which only uses the feature maps from the final C5 layer, nearly surpasses all other methods on all subsets. It only shows slightly worse results on the Hard subset as compared to the CMS-RCNN detector [40], which combines three *conv* feature maps of VGGNet [25].

Compared to the C5(16) model, adding the C4 feature maps slightly increases the performance on all subsets (refer to the 4th and 5th rows of Table 1). Moreover, connecting layers closer to the bottom of the network (C2 and C3) hardly produces any performance gain, except on the Hard subset. We can conclude that one branch models are designed specifically for the Easy and Medium subsets, but more effort needs to be made to improve their performance on the Hard subset. Therefore, in what follows, we use the skip connections of C4 and C5 as the optimal settings for

Table 1. Performance of our single branch models with different skip connections on the WIDER FACE validation set broken down into three subsets. The average precision (AP) results are reported. In the model CX(Y), X denotes which layer(s) is (are) used for skip connection and Y stands for the stride of the feature maps. The same annotation is used in Table 2 & 3.

Skip Connection	Easy	Medium	Hard
Multi-scale CNN [33]	0.711	0.636	0.400
Multi-task CNN [37]	0.851	0.820	0.607
CMS-RCNN [40]	0.902	0.874	0.643
C5(16)	0.920	0.887	0.640
C45(16)	0.921	0.888	0.643
C345(16)	0.921	0.888	0.645
C2345(16)	0.921	0.886	0.645

single branch models.

Although single branch models achieve surprising performance on the Easy and Medium subsets, the results on the Hard subset are far from satisfactory. Hence, we add another branch to detect faces with smaller spatial size. We summarize the detection results of these two branch models in Table 2. In this table, we observe that the C3(8)-C45(16) model (*i.e.* a model with one branch connected to C4 and C5, while the other branch connected to C3) shows significant improvement (more than 9% in absolute AP) over the C45(16) model on the Hard subset. This indicates that feature maps with finer spatial resolution are helpful in detecting faces at lower resolution and that the added branch enables this improvement. However, for this comparison, the performance of the two branch model drops on the Easy subset. After checking the detection results, we find that this decrease is mainly caused by false positive results with high classification score, which are generated from the new branch (*i.e.* small false positive faces). The C3(8)-C45(16) model utilizes the less powerful C3 feature maps to represent the small objects, which is similar in spirit to SSD [19] and MSCNN [2]. When we up-sample the deep feature map C5 and connect it with the C3 features (leading to the C35(8)-C45(16) model), the performance on all three subsets increases, especially on the Medium and Hard subsets (the 1st and 2nd rows of Table 2). This demonstrates that the connections of both shallow and deep feature maps are powerful and representative for small faces. When the C4 feature maps are added, the performance improves only slightly (the 3rd and 2nd rows of Table 2). Moreover, adding the C2 feature maps does not improve performance at all.

From the above comparisons, we conclude that skip connections can increase the performance on faces at all scales. However, we should design the connections carefully for each branch rather than simply connecting *conv* feature maps of all layers. Therefore, we conclude that combining deep (and spatially coarse) feature maps with shallow (and spatially fine-grained) feature maps is the key to successful-

Table 2. AP results of our two branch models with different skip connections on the WIDER FACE validation set.

Skip Connection	Easy	Medium	Hard
C3(8)-C45(16)	0.911	0.888	0.735
C35(8)-C45(16)	0.917	0.905	0.782
C345(8)-C45(16)	0.918	0.907	0.783
C2345(8)-C45(16)	0.917	0.907	0.782

Table 3. Performance of our different branch models with different skip connection on the WIDER FACE validation set. The AP results are reported.

Skip Connection	Easy	Medium	Hard
C45(16)	0.921	0.888	0.643
C345(8)-C45(16)	0.918	0.907	0.783
C345(8)-C45(16)-C45(32)	0.916	0.905	0.774

ly detecting faces at small scales.

4.3. What is the optimal number of branches?

In [2], the authors claim that the inconsistency between the sizes of objects and receptive fields compromises detection performance. Therefore, they add extra layers with large receptive fields to detect objects at large scale. However, there is no gain in performance when we add extra branches, as shown in Table 3. The reason might be that the deep C5 feature maps are of large receptive fields and are already representative for face detection, as compared to generic object detection [19, 2]. In fact, detection performance degrades, when a third branch is added (refer to last row of Table 3). This is most probably due to issues in training such a large network. Finding a favorable setting for all the hyper-parameters in this case is challenging. Therefore, we argue that two branches are enough for face detection and, unlike SSD [19] and MS-CNN [2], no extra branches are needed. So, in what follows, our MB-FCN detector is chosen to be the two branch C345(8)-C45(16) model.

4.4. Evaluation on FDDB [11]

The FDDB dataset [11] is a challenging benchmark for face detection. And it is arguably the most popular benchmark for face detection and nearly all state-of-art face detectors have been tested on it. FDDB only uses precision at specific false positive rates rather than AP (average precision) to evaluate detectors, which is not necessarily the most comprehensive way of evaluating detection performance. However, we follow convention and use this metric to compare with other methods. There are 67 unlabeled faces in FDDB [3], making precision not accurate at small false positive rates (*e.g.* @100fp). Hence, we report the precision rate at 500 false positives. Our MB-FCN detector (*i.e.* the C345(8)-C45(16) two branch model) achieves a superior performance over all other CNN-based detectors.

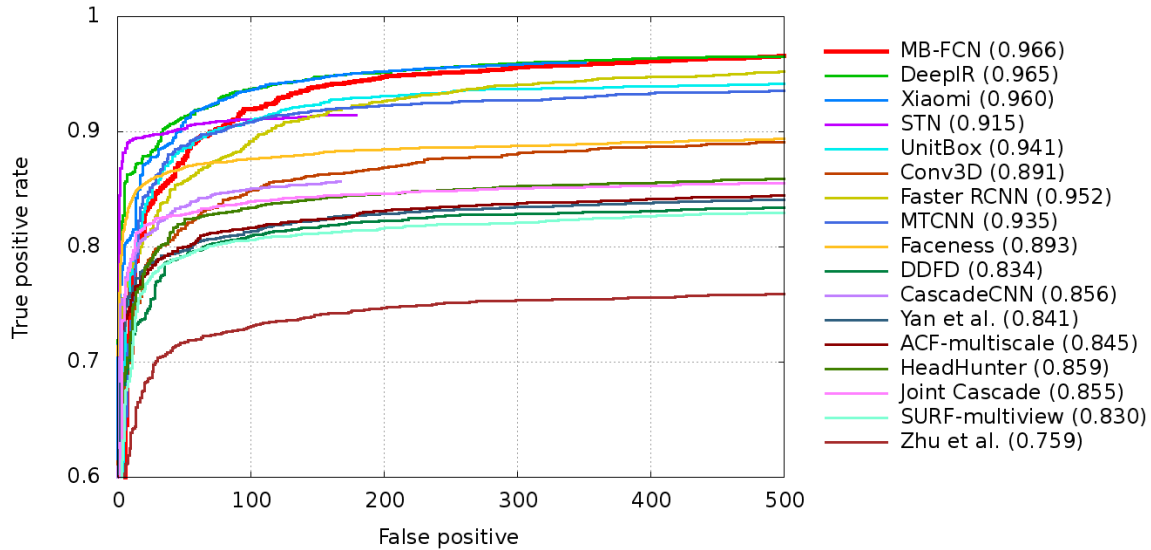


Figure 3. On the FDDB dataset, we compare our MB-FCN detector against many state-of-the-art methods: DeepIR [26], Xiaomi [28], STN [3], UnitBox [34], Conv3D [18], Faster RCNN [13], MTCNN [37], Faceness [32], DDFD [6], CascadeCNN [16], Yan *et al.* [29], ACF-multiscale [31], HeadHunter [21], Joint Cascade [4], SURF-multiview [17] and Zhu *et al.* [41]. The precision rate with 500 false positives is reported in the legend. The figure is best viewed in color.

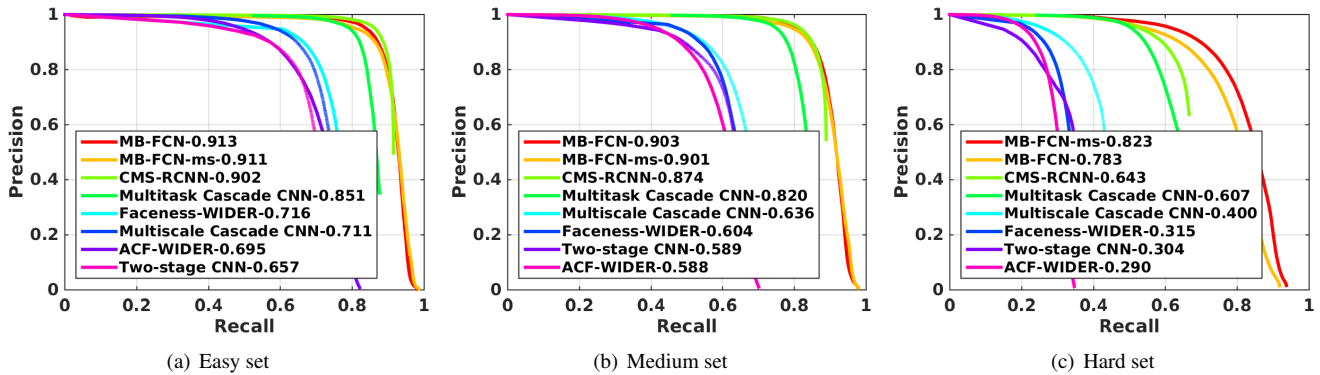


Figure 4. On the WIDER FACE dataset, we compare our MB-FCN detector against several state-of-the-art methods: CMS-RCNN [40], Multi-task Cascade CNN [37], Faceness-WIDER [32], Multi-Scale Cascade CNN [33], Two-Stage CNN [33], and ACF-WIDER [31]. The average precision (AP) results are reported in the legend. The figure is best viewed in color.

These results are shown in Figure 3. Moreover, the MB-FCN detector even surpasses all other detectors in precision at small false positive rates (*e.g.* @100-400fp) except the Xiaomi [28] and DeepIR [26] detectors. However, both of them are trained on WIDER FACE and fine-tuned on FDDB, while MB-FCN is only trained on WIDER FACE.

4.5. Evaluation on WIDER FACE [33]

Now, we apply our MB-FCN detector to the testing set of WIDER FACE. The results of the Easy/Medium/Hard testing subsets are shown in Figure 4. We see that the proposed MB-FCN detector surpasses all the methods on all subsets especially for the Hard subset, which is by far the most challenging. In comparison, CMS-RCNN [40] is a variant of Faster RCNN [13], which utilizes multi-layer *conv* feature

maps and context information to detect faces with low resolution. Compared to CMS-RCNN, MB-FCN achieves slightly better (+1.2%, +2.9%), and much better performance (+14.0%) on the Easy, Medium, and Hard subsets respectively. In fact, the improvement is quite significant on the latter subset, which further motivates our multi-branch approach capable of accurate face detection at small scales. We also test our MB-FCN detector on a coarse-level image pyramid (*i.e.* the input image is sampled at different scales and pushed through MB-FCN several times), which is a strategy used by previous face detectors. We denote this strategy as MB-FCN-ms. It is not surprising to see that it achieves better (+4.0%) performance than MB-FCN on the Hard subset, while running about five times slower.

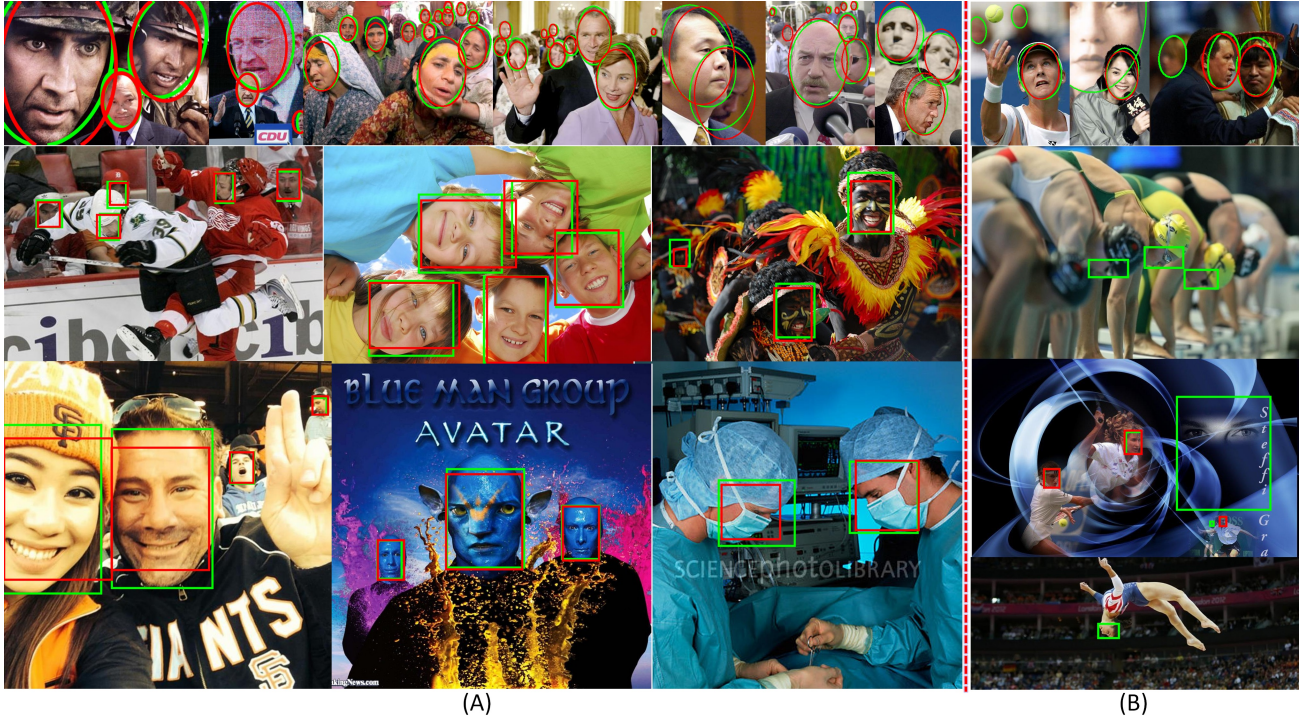


Figure 5. Some example results of the proposed MB-FCN face detector. Bounding boxes with green or red color are ground-truth annotations and MB-FCN detection results, respectively. (A) From the successful cases, we see that MB-FCN can deal with faces with extreme poses, large scale variations, exaggerated expressions, severe makeup and occlusion; (B) Some faces with extreme pose, severe truncation, or low resolution can still cause failures for MB-FCN.

4.6. Runtime Evaluation

One of the important advantages of our MB-FCN detector is its efficiency in dealing with faces in a wide range of possible scales. During the detection process, an image passes through the backbone network in only one single shot, which is more efficient than other methods that use an image pyramid. CascadeCNN [16, 37] is also designed with efficiency in mind and it runs at 100 FPS on a GPU for VGA (640×480 pixels) images. However, this speed is reported based on the assumption that it only encounters faces with resolution higher than 80×80 pixels. With this assumption, many faces with lower resolution would be missed, which is especially the case in the WIDER FACE dataset and in real-world applications. Decreasing the minimum detectable face size in CascadeCNN quickly increases the runtime of this method¹. Currently, our detector runs at 15 FPS on VGA images with no assumption on the minimum detectable face size. Moreover, the fast version of the STN detector [3] runs at about 30 FPS on VGA images. However, it only handles faces larger than 36×36 pixels and the ROI convolution is used to speed up the detector with minimal impact on the recall. As such, ROI convolution can also

¹On a workstation with Intel CPU E5-2698 and NVIDIA TITAN X GPU, CascadeCNN runs at 46, 20, and 10 FPS at a minimum detectable face size of 80×80 , 20×20 and 10×10 pixels, respectively.

be employed to further accelerate our detector.

4.7. Qualitative Results

We show some qualitative face detection results on sample images in Figure 5. From Figure 5(A), we observe that our MB-FCN detector can deal with challenging cases that have extreme poses, large scale variations, exaggerated expressions, severe makeup, and occlusion. However, Figure 5(B) also shows some failure cases, which are caused by very challenging nuisances. These results indicate that more progress is needed to further improve face detection performance, both in accuracy as well as runtime.

5. Conclusion

In this paper, we propose a multi-branch fully convolutional network (MB-FCN) for face detection. In our detection system, each branch uses specific connections of different *conv* layers to represent faces and learn a separate branch FCN for specific scale ranges. More importantly, the MB-FCN detector can detect faces within all scale ranges in a single shot, which makes it computationally efficient as it runs at 15 FPS on VGA images. Our MB-FCN detector is evaluated on two public face detection benchmarks, including FDDB and WIDER FACE and achieves superior performance when compared to state-of-the-art face detectors.

References

- [1] S. Bell, C. L. Zitnick, K. Bala, and R. Girshick. Inside-outside net: Detecting objects in context with skip pooling and recurrent neural networks. *CVPR*, 2016.
- [2] Z. Cai, Q. Fan, R. S. Feris, and N. Vasconcelos. A unified multi-scale deep convolutional neural network for fast object detection. In *ECCV*, 2016.
- [3] D. Chen, G. Hua, F. Wen, and J. Sun. *Supervised Transformer Network for Efficient Face Detection*. Springer, 2016.
- [4] D. Chen, S. Ren, Y. Wei, X. Cao, and J. Sun. Joint cascade face detection and alignment. In *ECCV*. Springer, 2014.
- [5] N. Dalal and B. Triggs. Histograms of oriented gradients for human detection. In *CVPR*. IEEE, 2005.
- [6] S. S. Farfade, M. J. Saberian, and L.-J. Li. Multi-view face detection using deep convolutional neural networks. In *ICM-R*. ACM, 2015.
- [7] R. Girshick. Fast r-cnn. In *ICCV*, 2015.
- [8] R. Girshick, J. Donahue, T. Darrell, and J. Malik. Rich feature hierarchies for accurate object detection and semantic segmentation. In *CVPR*, 2014.
- [9] B. Hariharan, P. Arbeláez, R. Girshick, and J. Malik. Hypercolumns for object segmentation and fine-grained localization. In *CVPR*, 2015.
- [10] K. He, X. Zhang, S. Ren, and J. Sun. Deep residual learning for image recognition. In *CVPR*, 2016.
- [11] V. Jain and E. G. Learned-Miller. Fddb: A benchmark for face detection in unconstrained settings. *UMass Amherst Technical Report*, 2010.
- [12] Y. Jia, E. Shelhamer, J. Donahue, S. Karayev, J. Long, R. Girshick, S. Guadarrama, and T. Darrell. Caffe: Convolutional architecture for fast feature embedding. In *ACM MM*, 2014.
- [13] H. Jiang and E. Learned-Miller. Face detection with the faster r-cnn. *arXiv*, 2016.
- [14] K. H. J. S. Jifeng Dai, Yi Li. R-FCN: Object detection via region-based fully convolutional networks. *NIPS*, 2016.
- [15] A. Krizhevsky, I. Sutskever, and G. E. Hinton. Imagenet classification with deep convolutional neural networks. In *NIPS*, 2012.
- [16] H. Li, Z. Lin, X. Shen, J. Brandt, and G. Hua. A convolutional neural network cascade for face detection. In *CVPR*, 2015.
- [17] J. Li and Y. Zhang. Learning surf cascade for fast and accurate object detection. In *CVPR*, 2013.
- [18] Y. Li, B. Sun, T. Wu, and Y. Wang. *Face Detection with End-to-End Integration of a ConvNet and a 3D Model*. Springer, 2016.
- [19] W. Liu, D. Anguelov, D. Erhan, C. Szegedy, S. Reed, C.-Y. Fu, and A. C. Berg. *SSD: Single Shot MultiBox Detector*. Springer, 2016.
- [20] J. Long, E. Shelhamer, and T. Darrell. Fully convolutional networks for semantic segmentation. In *CVPR*, 2015.
- [21] M. Mathias, R. Benenson, M. Pedersoli, and L. Van Gool. Face detection without bells and whistles. In *ECCV*. Springer, 2014.
- [22] H. Qin, J. Yan, X. Li, and X. Hu. Joint training of cascaded cnn for face detection. In *CVPR*, 2016.
- [23] S. Ren, K. He, R. Girshick, and J. Sun. Faster r-cnn: Towards real-time object detection with region proposal networks. In *NIPS*, 2015.
- [24] A. Shrivastava, A. Gupta, and R. Girshick. Training region-based object detectors with online hard example mining. *CVPR*, 2016.
- [25] K. Simonyan and A. Zisserman. Very deep convolutional networks for large-scale image recognition. *ICLR*, 2014.
- [26] X. Sun, P. Wu, and S. C. H. Hoi. Face detection using deep learning: An improved faster RCNN approach. *CoRR*, 2017.
- [27] P. Viola and M. J. Jones. Robust real-time face detection. *IJCV*, 2004.
- [28] S. Wan, Z. Chen, T. Zhang, B. Zhang, and K.-k. Wong. Bootstrapping face detection with hard negative examples. *arXiv*, 2016.
- [29] J. Yan, Z. Lei, L. Wen, and S. Li. The fastest deformable part model for object detection. In *CVPR*, 2014.
- [30] J. Yan, X. Zhang, Z. Lei, and S. Z. Li. Real-time high performance deformable model for face detection in the wild. In *ICIB*. IEEE, 2013.
- [31] B. Yang, J. Yan, Z. Lei, and S. Z. Li. Aggregate channel features for multi-view face detection. In *IJCB*. IEEE, 2014.
- [32] S. Yang, P. Luo, C.-C. Loy, and X. Tang. From facial parts responses to face detection: A deep learning approach. In *ICCV*, 2015.
- [33] S. Yang, P. Luo, C. C. Loy, and X. Tang. Wider face: A face detection benchmark. In *CVPR*, 2016.
- [34] J. Yu, Y. Jiang, Z. Wang, Z. Cao, and T. Huang. Unitbox: An advanced object detection network. In *MM*. ACM, 2016.
- [35] S. Zafeiriou, C. Zhang, and Z. Zhang. A survey on face detection in the wild: Past, present and future. *CVIU*, 2015.
- [36] S. Zagoruyko, A. Lerer, T.-Y. Lin, P. O. Pinheiro, S. Gross, S. Chintala, and P. Dollár. A multipath network for object detection. *BMVC*, 2016.
- [37] K. Zhang, Z. Zhang, Z. Li, and Y. Qiao. Joint face detection and alignment using multitask cascaded convolutional networks. *IEEE SPL*, 2016.
- [38] L. Zhang, L. Lin, X. Liang, and K. He. *Is Faster R-CNN Doing Well for Pedestrian Detection?* Springer, 2016.
- [39] B. Zhou, A. Lapedriza, J. Xiao, A. Torralba, and A. Oliva. Learning deep features for scene recognition using places database. In *NIPS*, 2014.
- [40] C. Zhu, Y. Zheng, K. Luu, and M. Savvides. Cms-rcnn: Contextual multi-scale region-based cnn for unconstrained face detection. *arXiv*, 2016.
- [41] X. Zhu and D. Ramanan. Face detection, pose estimation, and landmark localization in the wild. In *CVPR*. IEEE, 2012.